



## City Research Online

### City, University of London Institutional Repository

---

**Citation:** Jiang, H., He, L., Zhang, Q. & Wang, L. (2018). On scaling method to investigate high-speed over-tip-leakage flow at low-speed condition. *Journal of Engineering for Gas Turbines and Power*, 140(6), 062605. doi: 10.1115/1.4038619

This is the accepted version of the paper.

This version of the publication may differ from the final published version.

---

**Permanent repository link:** <https://openaccess.city.ac.uk/id/eprint/19480/>

**Link to published version:** <https://doi.org/10.1115/1.4038619>

**Copyright:** City Research Online aims to make research outputs of City, University of London available to a wider audience. Copyright and Moral Rights remain with the author(s) and/or copyright holders. URLs from City Research Online may be freely distributed and linked to.

**Reuse:** Copies of full items can be used for personal research or study, educational, or not-for-profit purposes without prior permission or charge. Provided that the authors, title and full bibliographic details are credited, a hyperlink and/or URL is given for the original metadata page and the content is not changed in any way.

---

---

---

City Research Online:

<http://openaccess.city.ac.uk/>

[publications@city.ac.uk](mailto:publications@city.ac.uk)

---

## ON SCALING METHOD TO INVESTIGATE HIGH-SPEED OVER-TIP-LEAKAGE FLOW AT LOW-SPEED CONDITION

**Hongmei Jiang**

University of Michigan-Shanghai Jiao Tong  
University Joint Institute, Shanghai Jiao Tong  
University, Shanghai, China

**Li He**

University of Oxford  
Oxford, UK

**Qiang Zhang**

City, University of London  
London, UK

**Lipo Wang**

University of Michigan-Shanghai Jiao Tong  
University Joint Institute, Shanghai Jiao Tong  
University, Shanghai, China

### ABSTRACT

Modern High Pressure Turbine (HPT) blades operate at high speed conditions. The Over-Tip-Leakage (OTL) flow can be high-subsonic or even transonic. From the consideration of problem simplification and cost reduction, the OTL flow has been studied extensively in low speed experiments. It has been assumed a redesigned low speed blade profile with a matched blade loading should be sufficient to scale the high speed OTL flow down to the low speed condition. In this paper, the validity of this conventional scaling approach is computationally examined. The CFD methodology was firstly validated by experimental data conducted in both high and low speed conditions. Detailed analyses on the OTL flows at high and low speed conditions indicate that, only matching the loading distribution with a redesigned blade cannot ensure the match of the aerodynamic performance at the low speed condition with that at the high-speed condition. Specifically, the discrepancy in the peak tip leakage mass flux can be as high as 22%, and the total pressure loss at the low speed condition is 6% higher than the high speed case. An improved scaling method is proposed hereof. As an additional dimension variable, the tip clearance can also be “scaled” down from the high speed to low speed case to match the cross-tip pressure gradient between pressure and suction surfaces. The similarity in terms of the overall aerodynamic loss and local leakage flow distribution can be improved by adjusting the tip clearance, either uniformly or locally.

### INTRODUCTION

The Over-Tip-Leakage (OTL) flow has a significant impact on the overall turbine aerodynamic performance. Many experimental studies have been carried out to study its complex flow physics and to validate various tip design concepts. During the design process of these experiments, the key flow conditions in the real engine have to be carefully scaled and matched, although there has always been a compromise between experimental accuracy and cost.

As a reasonable simplification which requires few compromises to represent the real blade structure [1], low speed linear cascades rigs have been widely used. The advantage of

these rigs are relatively low experimentation costs and excellent spatial resolution [1, 2]. In addition to match the Reynolds number and key geometry parameters, the blade profile employed in these low speed tests has to be redesigned to compensate the influence of compressibility at the high speed condition, so the blade loading could also be closely matched.

The scaling method related to the blade profile redesign has been well-studied in the literature. Wisler [3-5] studied pressure loss reduction in axial-flow compressors through Low-Speed Model Testing (LSMT) of GE-E3. The idea is to modify the incidence angles, the chordwise camber distributions, and the thickness distributions of the low-speed airfoils until these airfoils achieve the same normalized surface velocity distributions as the high-speed airfoils. The low-speed airfoils require leading edge camber line bending and somewhat thicker shape in order to match the velocity distributions. Low speed experiments by Lyes et al. [6–8] focused on the fourth stage of a five-stage high pressure compressor C147. The low speed blading was designed for same enthalpy rise across the rotor, and same non-dimensional axial velocity and absolute flow angle for the inlet to the rotor. A drawback is that the De Haller number (the blade exit-to-inlet velocity ratio) cannot be maintained. However, by designing the blade sections to produce the same distributions of normalized local velocity, the blade surface static pressure distributions is maintained. Vera and Hodson [9] studied the LP turbine blade-wake interaction at different conditions as low speed, high speed, steady and unsteady flow. To design the low speed blade profile, they first maintained the Reynolds number, and choose the exit angle and the ratio of inlet to exit Mach number (velocity) as close as possible to the corresponding high speed values in the engine. The inlet angle and the shape of the blade were modified to take into account of the compressibility effect as well as the stream tube divergence. González P. et al. [10] redesigned a high-lift low-pressure turbine blade, and more attention was paid to effect of blade thickness on the profile loss. Their low speed experiment with the same Reynolds number aimed to ensure the dynamic similarity. Gallimore et al. [11, 12] conducted high-speed and low-speed testings of sweep and dihedral technology on the multistage axial flow compressor of

the Trent engine. Although the design point parameters were not exactly the same as those for the high-speed compressor, their results show that 3D blading was effective and promising. Zhang et al. [13, 14] reported the separation and transition control based on the high speed and low speed tests of the HSU2 airfoil, especially for the effects of unsteadiness and surface roughness. The low-speed and high-speed profiles were redesigned to have the same normalized isentropic Mach number distribution by reducing the inlet angle of the low-speed profile. In the low speed test for the High-Lift LP turbine airfoils, Michele et al. [15] modified the airfoil to match the isentropic velocity ratio and isentropic Mach ratio for T106C at the same Reynolds number by changing pitch to axial chord ratio, the ideal incompressible Zweifel number, the diffusion rate and outflow angle. From the modeling consideration, Wang et al. [16–18] kept the same geometrical scaling principles (consistence, aspect ratio and hub to tip ratio) and aerodynamic principles (discharge coefficient, pressure rise coefficient, vector graphics component, loss coefficient, reaction degree and blade surface pressure coefficient) to model the high speed flow field.

There have also been some very recent studies addressing the three-dimensional blading redesign. The high-to-low speed transformation process involves both geometric and aerodynamic considerations. For high-pressure compressor blades, low speed testing models were redesigned and implemented by Zhang et al. [19], Zhang et al. [20]. Their designed LSMT was used to optimize the 3D blade for LSMT [21]. Giovannini et al. [22] scaled the three-dimensional low-pressure turbine blades for the low-speed testing. The 3D blade loading distribution between the real engine environment and their low speed facility was matched, which then led to a comparable behavior of the boundary layer and hence the profile losses.

The majority of previous blade tip aerodynamic studies have been conducted at low speed conditions and similar scaling method has been adopted. One default assumption was that the major tip flow structures at high speed condition could be reproduced by a redesigned low speed blade with a matched loading. Wheeler et al. [23] reported different flow structures at high and low speed conditions, especially when the tip flow accelerates to a supersonic regime and involves shock structures. However, even without the impact of shock waves on the OTL, it still remains unclear if the conventional scaling method would work for high subsonic conditions.

In this paper, the validity of the conventional scaling method for studying the OTL flow will be studied. A low speed blade profile was redesigned to match the blade loading at a high speed condition. Detailed analyses, including the aerodynamic loss, leakage mass flow rate, and the OTL flow structure at high and low speeds are then presented. A more practical scaling method is proposed for future low speed OTL experimental studies.

## NUMERICAL SETUP AND VALIDATION

A commercial CFD solver, ANSYS FLUENT 14.5, was employed in the present numerical study. This software solves the 3D, steady, turbulent form of the Reynolds-averaged Navier–Stokes (RANS) equations with a finite volume method. Two-equation turbulence model, K-Omega shear stress transport (SST) was chosen for solving all the cases in the present study. Figure 1 presents the 3D computational domain and meshes employed in the present study. The computational domain consists of one single HPT blade with periodic boundary conditions. The same blade profile was employed by Ma et al. [24] in a high speed experimental study. A commercial meshing software, POINTWISE, was employed to generate 2D and 3D structured meshes.

Grid-independence study was performed, and special attention was paid on the grids density (near-wall grid size/expansion ratio) in the tip gap. For all the cases, average  $y^+$  value on tip surfaces is less than 1 to resolve the near wall boundary layer. The grid information and averaged results are listed in Table 1. Figure 2 shows local OTL mass flux distribution obtained with three density levels of grids (2.4 million, 3.8 million, and 5.2 million) at a location near the exit of the tip region. The differences in the averaged OTL mass flow rate are negligible between 3.8 million and 5.2 million grids. Therefore, 3.8 million grids mesh was chosen for all the 3D calculations in this numerical study.

With the computational setup mentioned above, satisfactory agreements between experimental and CFD results have been reported by previous tip studies by Ma et al. [25,26]. Further validations of the CFD performance on tip heat transfer at the high speed (exit Mach number 0.86) and a low speed condition (exit Mach number 0.45) are presented in Fig. 3. The experimental tip HTC contour shown in Fig 3a was produced with the same experimental data by Ma et al [24] in a high speed condition. The experimental methods and uncertainty analysis were detailed by Ma et al. [24] and Ma et al [25]. The overall trend and local variations are very different between high speed flow (Fig. 3a) and low speed flow (Fig. 3b). Higher heat transfer regions are located in the frontal region of the tip surface and the pressure side edge (due to a flow reattachment and cross-flow diffusion).

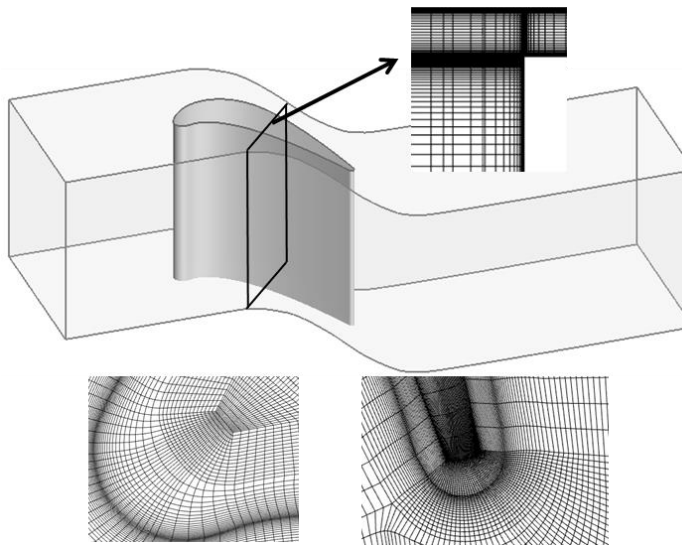


Fig. 1: Setup of the computational domain and mesh.

Table 1 Mesh Independence Study

Grid Size	2.4 million	3.8 million	5.2 million
Grid Points within Tip Gap	20	40	70
Non-dimensional Mass flow rate	0.0406	0.0408	0.0409

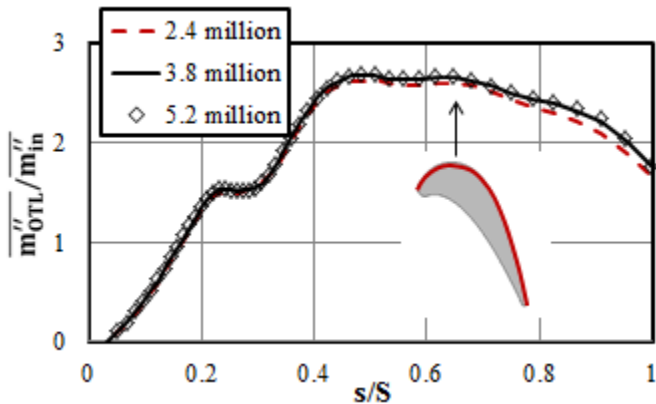


Fig. 2: Convergence of the non-dimensional radially averaged OTL mass flux distribution on the suction side edge with different grid points.

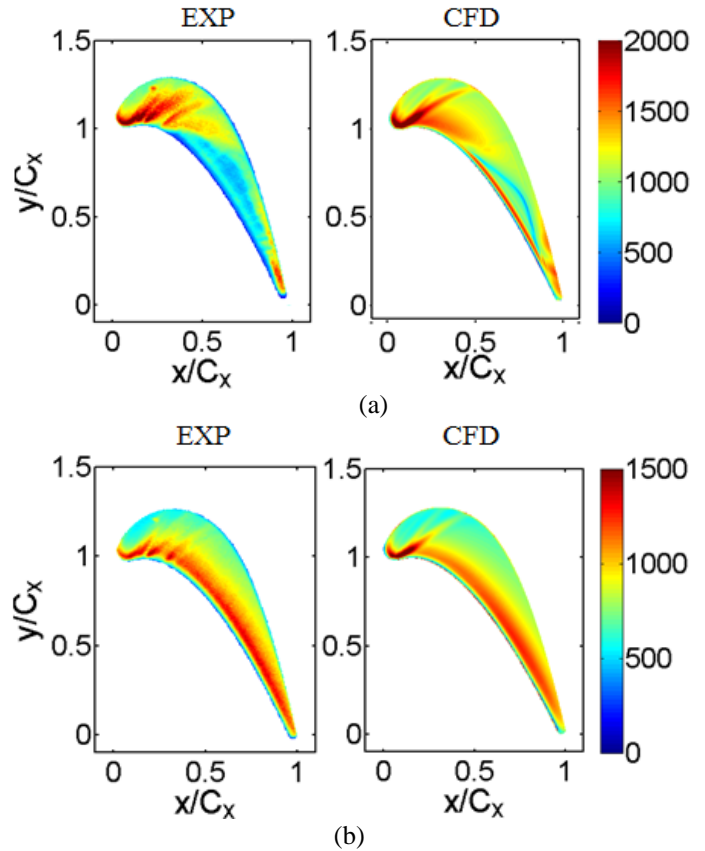


Fig. 3 Contours of HTC (a) high speed case,  $P_{0,1}/P_{s,2}=1.8$ ,  $M_2=0.86$ , (b) low speed case,  $P_{0,1}/P_{s,2}=1.2$ ,  $M_2=0.45$ .

### HIGH-TO-LOW SPEED BLADE REDESIGN TO MATCH LOADING

To obtain the dynamic similarity of high speed and low speed flow, the Reynolds number, inlet flow angle, pitch to axial chord ratio and span to axial chord ratio are kept invariant in the scaling process. For the high speed case the outlet Mach number is about 0.60, while for the low speed case the outlet Mach number is about 0.09. For both cases the same Reynolds number is set as  $Re=6.4 \times 10^5$ . For baseline case of high speed flow investigated in the present study, the tip clearance height ( $G$ ) is equivalent to 1% of the blade span (a typical engine design value).

The redesigned low speed blade profile and the original high speed one are shown in Fig. 4, respectively. The profile scaling process involves shape parameterization with multiple control points on spline curve. An increase in blade thickness and modification in blade camber line are also involved. The trailing edge thickness-to-chord ratio was kept as constant to ensure no significant increase in the trailing-edge loss. The detailed profile scaling process is presented in Fig. 5. The objective function to the relative root mean square error with respect to the averaged high speed blade load:

$$RRMS = \frac{\left\{ \frac{1}{N} \sum_{i=1}^N [f_{LS}(i) - f_{HS}(i)]^2 \right\}}{\frac{1}{N} \sum_{i=1}^N f_{HS}(i)} \quad (1)$$

where N is the number of control points,  $f = M_s/M_2$ .

Figure 6a presents mid-span normalized isentropic Mach number  $M_s/M_2$  distributions for the high and low speed cases. The high speed blade becomes front-loaded if running at low speed without redesign. The relative error of high speed profile between high speed and low speed conditions can reach 14%, while the high speed profile and low speed profile have load discrepancy of less than 1% after the redesign. Figure 6b also indicates the difference of relative Mach number  $M/M_2$  distribution in middle span is negligible.

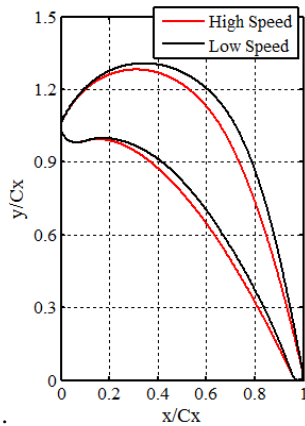


Fig. 4 Original high speed blade profile and redesigned low speed blade profile.

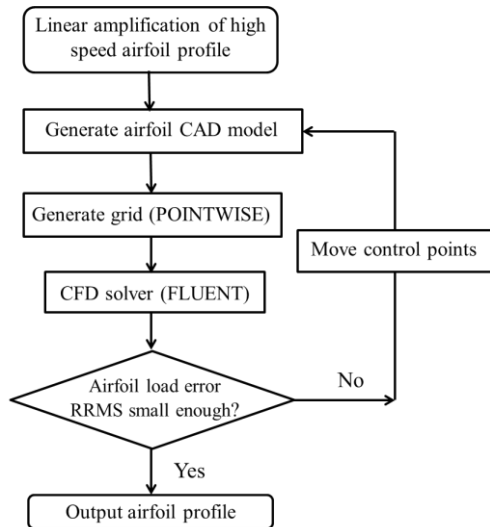


Fig. 5 Profile scaling process.

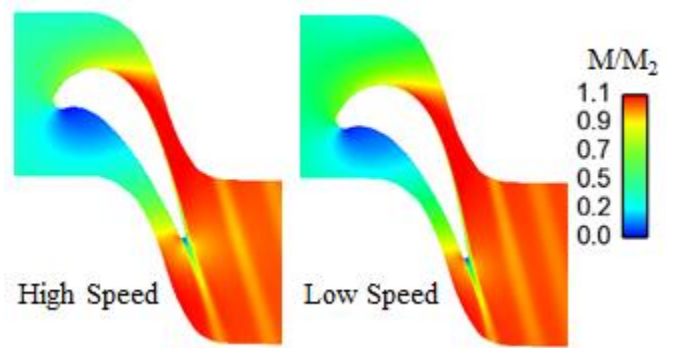
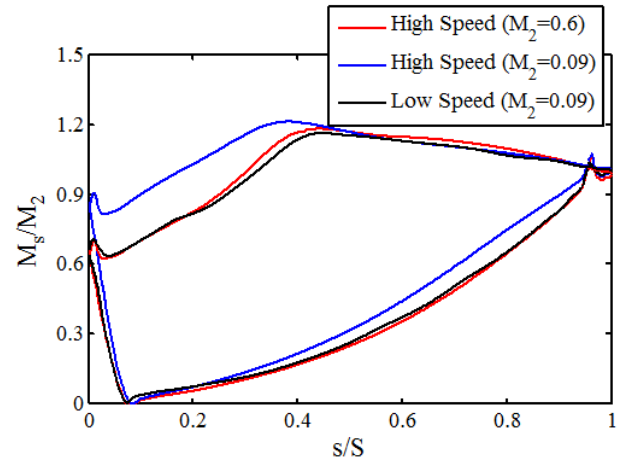


Fig. 6 Normalized Mach number distribution at middle span, (a) isentropic Mach number along blade surface, (b) Mach number contour.

### SCALING ISSUE WITH TIP LEAKAGE FLOW

The scaling performance particularly in tip leakage flow is the focus of this section's discussions. Normalized mass flux contour on a curved cut plane at the tip gap exit is illustrated in Fig. 7. For both high and low speed cases, higher leakage flow occurs over the rear half of the blade tip surface. Compared with the original high speed condition, the low speed case shows a much higher amount leakage flow, with a same tip gap to span ratio and blade mid-span loading. Figure 8 shows the distribution of non-dimensional leakage mass flow rate  $\dot{m}_{tip,local}$ , which is defined as local leakage mass flow rate relative to the passage flow rate,

$$\dot{m}_{tip,local} = S \int_0^G r v_n dz / m_{passage} \quad (2)$$

Consistently the leakage flow of low speed redesigned blade is more intense than the high speed case, especially at  $s/S=0.6\sim 1$ . The maximum difference, which is about 22%, appears in  $s/S=0.52$ . Radially-averaged leakage mass flow vectors are further illustrated in Fig. 9.

The OTL flow is driven by the pressure difference across the tip region from the pressure side to suction side. The magnitude of leakage flow rate is determined by the pressure gradient across the tip. Fig. 10 presents the pressure coefficient  $C_p$  contour on a streamwise cut plane at  $s/S=0.6$ . Relative speaking, the pressure gradient over the low speed blade is much larger than the high speed blade. Considerable larger separation bubble can be observed in the low speed condition.

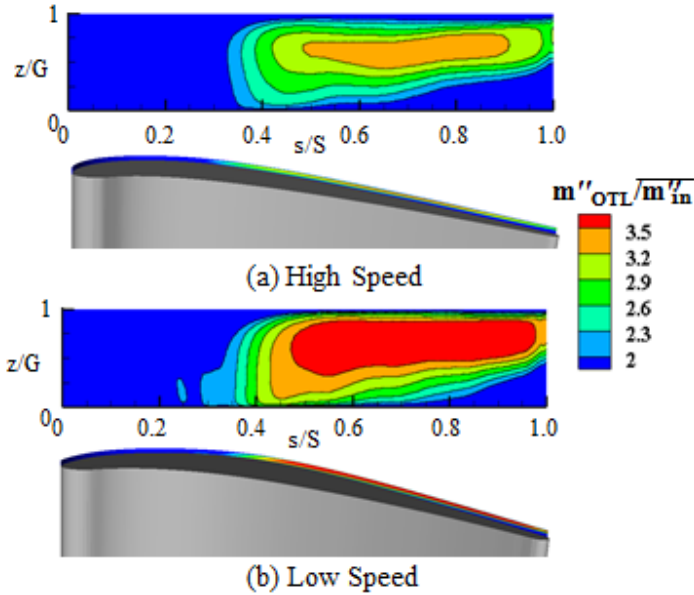


Fig. 7 Mass flux ratio distribution at tip region above the suction side edge, (a) High Speed, (b) Low Speed.

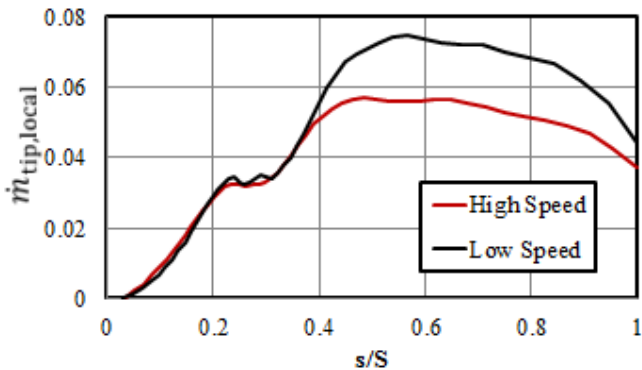


Fig. 8 Comparison of normalized local tip leakage mass flow rate along suction-side curve length for the high speed and low speed cases.

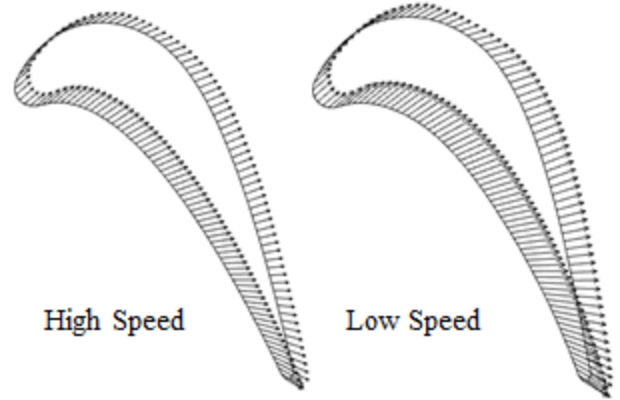


Fig. 9 Radially-averaged leakage mass flow vectors.

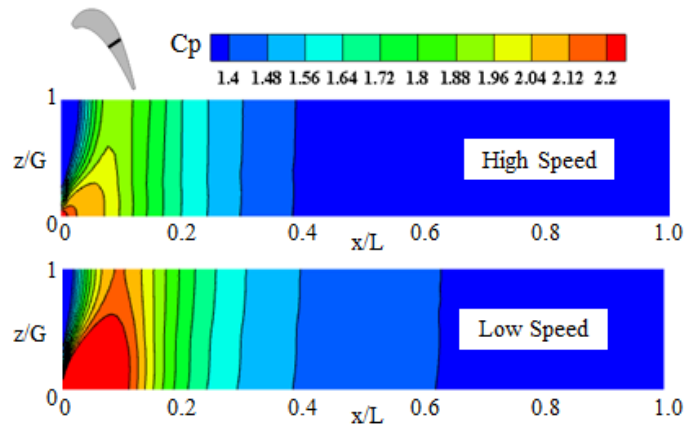


Fig. 10 Pressure coefficient  $C_p$  contours in the tip gap on the cut plane at  $s/S=0.6$  (as indicated).

The difference in the OTL mass flow between high speed and low speed cases will inevitably influences the total aerodynamic loss. Here, a normalized local total pressure-loss coefficient  $\xi$  is defined as

$$CP_0 = \frac{P_{01} - P_0}{0.5\rho_2 v_2^2} \quad (3)$$

$$\xi = \frac{CP_0}{\overline{CP}_{0,passage}} \quad (4)$$

where  $CP_0$  is the local total pressure loss normalized by the exit dynamic head, and  $\overline{CP}_{0,passage}$  is the overall mass-averaged total pressure loss for the whole passage. Figure 11 shows the distribution of  $\xi$  in the entire passage. At the low speed condition, the tip leakage loss core is larger in size and the relative tip leakage loss is much higher.

An OTL loss coefficient is defined as,

$$\overline{CP}_{0tip} = \frac{\overline{CP}_{0passage}}{\overline{CP}_{0passage,withoutgap}} \quad (5)$$

For each case, an extra zero tip gap case was calculated to account for the aerodynamic loss without leakage flow. Table 2 lists the loss breakdown. The normalized OTL average loss coefficient for low speed condition is 6 percent higher than the original high speed case.

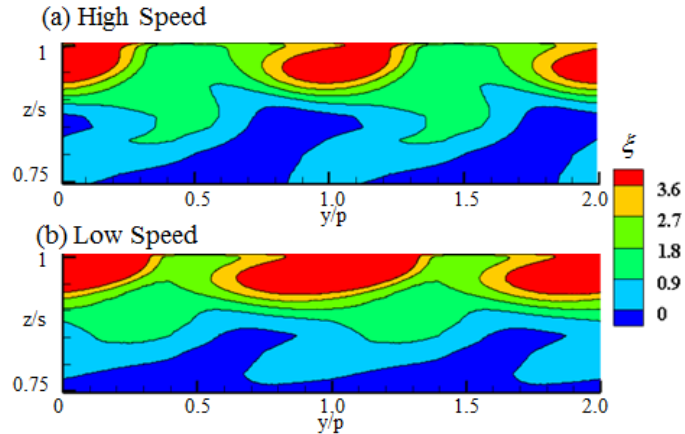


Fig. 11 Normalized local total pressure loss coefficient contour at 2 Cx cut plane (a) High Speed, (b) Low Speed.

Table 2 Averaged aerodynamic losses for High Speed and Low Speed

	High Speed	Low Speed
$\overline{CP}_{0\text{passage}}$	0.1932	0.1743
$\overline{CP}_{0\text{passage\_withoutgap}}$	0.0966	0.0851
$\overline{CP}_{0\text{tip}}$	0.0966	0.0892
$\bar{\xi}_{\text{tip}} = \overline{CP}_{0\text{tip}} / \overline{CP}_{0\text{passage}}$	0.499	0.512

**A PRACTICAL METHOD: SCALING THE TIP GAP**

It seems low speed tip experimental research faces a scaling dilemma: a matched blade loading and tip leakage flow cannot be achieved at the same time. However, if the blade profile could be altered for matching loading, the tip gap height should also be allowed to be scaled for matching the pressure gradient which drives the leakage flow. Results shown in Figs. 6-10 indicate the low speed version of a “redesigned tip gap” should be smaller than the original high speed case.

Results for two more low speed case with smaller tip gap heights are shown in Figs. 12-15. The geometry information is shown in Fig. 12. One case has a uniformly reduced tip gap ratio (from 1% to 0.8%), the other one has a variable height along the axial direction.



Fig 12 “Scaled down” low speed tip gap height.

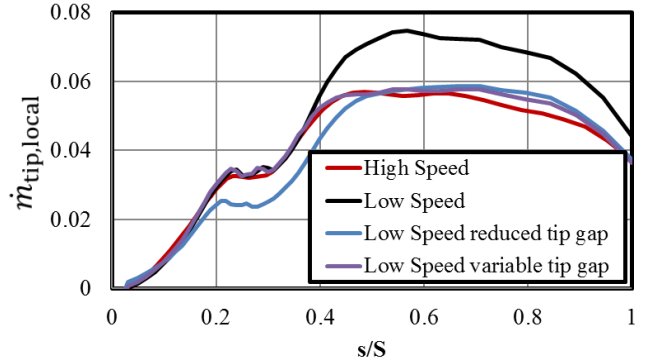


Fig. 13 Comparison of normalized local tip leakage mass flow rate along suction-side curve length for High Speed and Low Speed reduced tip gap.

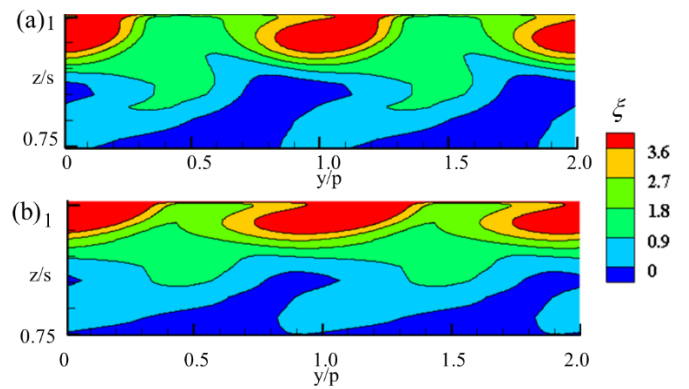
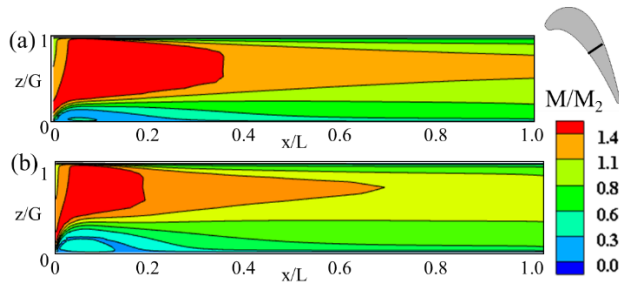


Fig. 14 Normalized local total pressure loss coefficient contour (a) High Speed, (b) Low Speed variable tip gap heights.

Distributions of local leakage mass flow rate ratio are shown in Fig. 13. A uniformly reduced gap height reduces the leakage flow in both frontal and rear regions. The undesired mismatching issue at the frontal region can be further improved by a variable height design. The overall averaged OTL mass flow rate ratio could be closely matched between high and low speed cases (0.0402 for reduced tip gap case and 0.0408 for high speed case).

Figure 14 shows normalized local total pressure loss coefficient contours. Scaling down the tip gap height reduces the tip leakage vortex in general, although the size and shape of the loss core are still not well matched due to the interactions between passage secondary flow and leakage flow. Normalized Mach number distributions shown in Fig 15 also illustrate different behaviours for separation bubbles in high and low speed flows. The high speed OTL flow is associated with a smaller separation bubble. It is still not an easy scaling process to obtain a full aerodynamic similarity.



**Fig. 15 Mach number distribution of cut plane  $s/S=0.52$  (a) High Speed, (b) Low Speed reduced tip gap.**

However, the results in the present study indicate that it is hopeful to improve the conventional tip gap scaling process with further efforts on optimization. With the same logical reasons for blade profile redesign, the tip gap height does not have to be uniformly scaled down. Variable tip gap height could achieve an improved matching performance with shape parameterization technique employed in profile matching process.

## CONCLUSIONS

The conventional scaling method to study high speed OTL flow in low speed experimental condition was numerically assessed in this study. Aerodynamic performance of a low speed redesigned blade was analyzed and compared with the results from the original high speed condition. The results from the present study demonstrate consistently that the blade mid-span loading and leakage flow structure cannot be both matched. Large discrepancies in the local leakage flow rate distribution and the overall aerodynamic loss were identified.

This study proposes a practical method: the tip gap height could also be scaled “down” in addition to redesigning the blade profile. An improved performance is observed with variable gap height scaling.

It is noted that the proposed method is still limited in resolving the dilemma in the high-to-low speed scaling. It could be hopeful to apply this method to study the aerodynamics of high subsonic OTL flow. However, it would be far more challenging, even if possible, to mimic complex transonic flow phenomena in the real engine condition, especially in terms of tip heat transfer studies.

## NOMENCLATURE

$C$	= blade chord (m)
$C_x$	= axial chord (m)
$C_p$	= pressure coefficient, $C_p = (P_{01} - P) / (P_{01} - P_2)$
$CP_0$	= local total pressure loss coefficient, $CP_0 = (P_{01} - P_0) / 0.5\rho V^2$
$\overline{CP_0}$	= mass-averaged total pressure loss coefficient
$G$	= tip gap height (m)
$M$	= Mach number
$P$	= Pressure (Pa)

$Re$	= axial chord and outlet velocity based Reynolds number
RRMS	= relative root mean square error
$S$	= total surface curve length (m)
$Tu$	= turbulence intensity
$V$	= velocity magnitude (m/s)
$m''$	= mass flux ( $\text{kg}/\text{m}^2$ )
$\dot{m}$	= mass flow rate (kg/s)
$\dot{m}$	= mass flow rate ratio
$s$	= curve length(m) , blade span (m), isentropic value
$\nu$	= dynamic viscosity ( $\text{kg}/\text{ms}^{-1}$ )
$x, y, z$	= Cartesian coordinates
$y^+$	= non-dimensional wall distance
$\zeta$	= normalized local total pressure loss coefficient, $CP_0 / \overline{CP_0}$
$\alpha_1$	= in flow angle ( $^\circ$ )
$\rho$	= density ( $\text{kg}/\text{m}^3$ )
<b>SUBSCRIPTS</b>	
$s$	= static
$0$	= total
$1$	= inlet
$2$	= outlet

## Acknowledgments

The authors gratefully acknowledge the support of Chinese National Science Foundation (51376127) for funding the study.

## REFERENCES

- [1] Hodson, H. P., and Dominy, R. G., 1993, “Annular Cascades,” Advanced Methods for Cascade Testing, AGARD-AG-328.
- [2] Wisler, D. C., 1984, “Loss Reduction in Axial Flow Compressors Through Low-Speed Model Testing,” ASME paper No. 84-GT-184.
- [3] Wisler, D. C., 1977, “Core Compressor Exit Stage Study, Volume I—Blading Design,” NASA CR No. 135391.
- [4] Wisler, D. C., 1985, “Loss Reduction in Axial-Flow Compressor Through Low-Speed Model Testing,” ASME J Gas Turb Pwr, 107(2), pp. 354–363.
- [5] Wisler, D. C., Halstead, D. E., and Beacher, B. F., 1999, “Improving Compressor and Turbine Performance Through Cost-Effective Low-Speed Testing,” 14th International Symposium on Air Breathing Engines, Florence, Italy, September 5–10, ISABE Paper No. 99-7073.
- [6] Lyes, P. A., and Ginder, R. B., 1998, “Experimental Evaluation of the High-to-Low Speed Transformation Process for a Highly Loaded Core Compressor Stage,” ASME Paper No. 98-GT-334.
- [7] Lyes, P. A., and Ginder, R. B., 1999, “Low-Speed Compressor Tests of Swept and Bowed Blade Designs,” ISABE Paper No. 99-7048.

- [8] Lyes, P. A., 1999, "Low Speed Axial Compressor Design and Evaluation: High Speed Representation and Endwall Flow Control Studies," Ph.D. thesis, Cranfield University, Cranfield, UK.
- [9] Vera, M., and Hodson, H. P., 2002, "Low-Speed Versus High-Speed Testing of LP Turbine Blade-Wake Interaction," 16th Symposium on Measuring Techniques in Transonic and Supersonic Flows in Cascades and Turbomachines, Cambridge, UK, Sept. 23–24, Paper No. 7-2.
- [10] González P., Ulizar I., Vázquez R., Hodson H. P., 2002, "Pressure and Suction Surfaces Redesign for High-Lift Low-Pressure Turbines," ASME J Turbomach, 124, pp. 161-166.
- [11] Gallimore, S. J., Bolger, J. J., Cumpsty, N. A., Taylor, M. J., Wright, P. I., and Place, J. M. M., 2002, "The Use of Sweep and Dihedral in Multistage Axial Flow Compressor Blading—Part I: University Research and Methods Development," ASME J Turbomach, 124(4), pp. 521–532.
- [12] Gallimore, S. J., Bolger, J. J., Cumpsty, N. A., Taylor, M. J., Wright, P. I., and Place, J. M. M., 2002, "The Use of Sweep and Dihedral in Multistage Axial Flow Compressor Blading—Part II: Low and High-Speed Designs and Test Verification," ASME J Turbomach, 124(4), pp. 533–541.
- [13] Zhang, X. F., Vera, M., Hodson, H. P., 2006, "Separation and Transition Control on an Aft-Loaded Ultra-High-Lift LP Turbine Blade at Low Reynolds Numbers: Low-Speed Investigation," ASME J Turbomach, 128, pp. 517-527.
- [14] Vera, M., Zhang, X. F., and Hodson, H. P., 2007, "Separation and Transition Control on an Aft-Loaded Ultra-High-Lift LP Turbine Blade at Low Reynolds Numbers: High-Speed Validation," ASME J. Turbomach., 129, pp. 340-347.
- [15] Marconcini, M., Rubecchini, F., Pacciani, R., Arnone, A., and Berini, 2012, "Redesign of High-Lift Low Pressure Turbine Airfoils for Low Speed Testing," ASME J Turbomach, 134(5), p. 051017.
- [16] Wang Z.Q., 2010, "Research on the Method of Low-Speed Model Testing for High Pressure Compressor," Ph.D. thesis, Nanjing University of Aeronautics and Astronautics, Nanjing, China.
- [17] Wang Z.Q., Hu J., Wang, Y.F., and Zhai, X.C., 2010, "Aerodynamic Design of Low-Speed Model Compressor for Low-Speed Model Testing," Acta Aeronaut. Astronaut. Sin., 31(4), pp. 715–723.
- [18] Wang Z.Q., Hu, J., Wang, Y.F., and Ruan, L.Q., 2012, "Low Speed Model Testing for High Pressure Compressor," Acta Aeronaut. Astronaut. Sin., 33(5), pp. 828–838.
- [19] Zhang, C.K., Hu, J., Wang, Z.Q., and Gao, X., 2014, "Design Work of a Compressor Stage Through High-To-Low Speed Compressor Transformation," ASME J Gas Turb Pwr, 136(6), p. 064501.
- [20] Zhang, C.K., Wang Z.Q., Yin, C., Yan, W., and Hu, J., 2014, "Low speed Model Testing Studies for an Exit Stage of High Pressure Compressor," ASME J. Eng. Gas Turbines Power., 136(11), p. 112603.
- [21] Zhang, C.K., Hu, J., Wang, Z.Q., and Li, J., 2016, "Experimental Investigations on Three-Dimensional Blading Optimization for Low-Speed Model Testing," ASME J Gas Turb Pwr, 138(12), p. 122602.
- [22] Giovannini, M., Marconcini, M., Rubecchini, F., Arnone, A., and Bertini, F., 2016, "Scaling Three-Dimensional Low-Pressure Turbine Blades for Low-Speed Testing," ASME J Turbomach, 138, p. 111001.
- [23] Ma, H., Wang, Z., Wang, L., Zhang, Q., Yang, Z., and Bao Y., 2015, "Ramp Heating in High-speed Transient Thermal Measurement with Reduced Uncertainty," ASME Paper No. GT2015-43012.
- [24] Wheeler, A. P. S., Atkins, N. R., and He, L., 2011, "Turbine Blade Tip Heat Transfer in Low Speed and High Speed Flows," ASME J Turbomach, 133(4), p. 041025.
- [25] Ma, H., Zhang, Q., He, L., Wang, Z., and Wang, L., 2016, "Cooling Injection Effect on A Transonic Squealer Tip - Part 1: Experimental Heat Transfer Results and CFD Validation," ASME J. Eng. Gas Turbines Power, GTP-16-1338, pp: 1-11.
- [26] Ma, H., Zhang, Q., He, L., Wang, Z., and Wang, L., 2016, "Cooling Injection Effect on A Transonic Squealer Tip - Part 2: Analyses of Aerothermal Interaction Physics," ASME J. Eng. Gas Turbines Power, GTP-16-1339, pp: 1-11.